Tunable Thermo-Responsive Poly(*N*-vinylcaprolactam) Cellulose Nanofibers: Synthesis, Characterization, and Fabrication[a,b]

Martial Webster, Jianjun Miao, Brandon Lynch, Da'Sean Green, Reginald Jones-Sawyer, Robert J. Linhardt,* Juana Mendenhall*

Temperature-responsive PVCL homopolymers and functional PVCL polymers containing carboxylic acids are prepared in organic and aqueous solutions. PVCL bulk polymers are characterized using ^{1}H NMR, photometry, ATR-FTIR, and thermal analysis. A finite phase transition at 37–40 °C occurs in aqueous solutions of PVCL and PVCL-COOH. PVCL and PVCL-COOH polymers are electrospun into fibers ranging from 100 to 2300 nm in diameter. PVCL/cellulose bi-component films are obtained by electrospinning of CA and PVCL followed by alkaline hydrolysis. These tunable thermo-responsive PVCL/cellulose nanofibers have potential applications in developing affinity membranes.

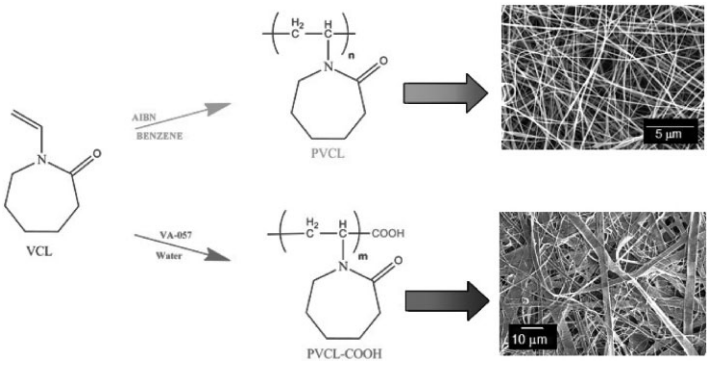

1. Introduction

Electrospinning is a technique to fabricate nano to μm-sized fibers from polymer solutions or melts. The resulting electrospun fibers have a variety of applications such as biomedical devices, filtration systems, chromatographic supports for protein separation, and affinity membranes for enzyme-based sensors.[1] Affinity membranes can be prepared from hydrophilic fibers such as cellulose fibers, which show minimal protein adsorption characteristics and can also be used along with hydrophobic smart materials.

Smart materials respond to external stimuli such as changes in pH, temperatures, anionic strength, electric fields, or light irradiation.[2,3] Temperature-responsive polymers are a class of smart materials that undergo a phase transition in aqueous solutions as temperatures surpass a certain point, which is characterized as the lower critical solution temperature (LCST).[4] At temperatures below the LCST, macromolecules swell while at temperatures above LCST macromolecules may collapse. These polymers are commonly used in the pharmaceutical and biotechnological applications such as drug delivery, tissue engineering, enzyme entrapment, membrane separation, and catalysis.[5,6]

One commonly investigated thermo-responsive polymer is poly(*N*-isopropylacrylamide) (PNIPAM) which displays an LCST in the range of 31–35 °C in aqueous solutions. The

M. Webster, B. Lynch, D. Green, R. Jones-Sawyer, J. Mendenhall
Department of Chemistry, Morehouse College, Atlanta, Georgia 30314, USA
E-mail: jmendenhall@morehouse.edu
J. Miao, R. J. Linhardt
Center for Biotechnology and Interdisciplinary Studies and Rensselaer Center for Nanotechnology, Department of Chemical and Biological Engineering, Rensselaer Polytechnic Institute, Troy, New York 12180, USA
E-mail: linhar@rpi.edu

[a] **Supporting Information** for this article is available from the Wiley Online Library or from the author.

[b] M. W. and J. M. contributed equally to this work.

DOI: 10.1002/mame.201200081

LCST of PNIPAM can be altered through the addition of surfactants and organic solvents.[7] At temperatures above the LCST, PNIPAM displays hydrophobic interaction with water molecules.[8] Extensive investigation of PNIPAM demonstrates that the LCST can be determined using a variety of methods such as turbidity, photometry, light scattering, differential scanning calorimetery, mathematical modeling, and infrared spectroscopy.[9] PNIPAM has the downside that it can be degraded into low-molecular-weight amines, which exhibit high cytotoxicity.[10] This adverse property limits the long-term use of PNIPAM in biotechnological applications. In contrast to PNIPAM, poly(*N*-vinylcaprolactam) (PVCL), another temperature-responsive polymer, shows promise in biotechnological applications. The presence of the amide group in PVCL reduces its susceptibility to degrade into low-molecular-weight products.[10] PVCL also exhibits a tunable LCST at 32–37 °C, which allows PVCL to be used in processes geared toward affinity precipitation for isolation, purification of proteins, the immobilization of enzymes, and catalysis.[11]

In this study, we synthesized two types of PVCL homopolymers, one PVCL with functional group on its chain end and another one without a functional group. The carboxyl-functionalized PVCL-3 was obtained by using 2,2′-azobis[*N*-(2-carboxyethyl)-2-methylpropionamidine]-hydrate (VA-057) as the initiator, and unfunctionalized PVCL-1 and PVCL-2 were prepared using 2,2′-azoisobutyronitrile (AIBN) as the initiator. These three PVCL homopolymers were subjected to electrospinning, resulting in electrospun fibers having unique morphologies. Mixtures of PVCL/cellulose acetate (PVCL-CA) fibers were also prepared through electrospinning to obtain composite fibers further hydrolyzed to yield PVCL/cellulose bi-component films.

2. Experimental Section

2.1. Materials and Methods

N-vinylcaprolactam (VCL), AIBN, and VA-057 were purchased from Sigma-Aldrich. CA ($\overline{M}_w$ 53 kDa, degree of acetylation 39.7%) and poly(ethylene oxide) ($\overline{M}_w$ 400 kDa) were obtained from Fisher Scientific. All solvents were purchased from Fisher Scientific and used without further purification. All solutions were prepared as weight per volume (w/v).

2.1.1. Polymerization of VCL

The following polymerizations were prepared similar to the procedures by Vihola et al.[12] and Boyko et al.[13] VCL was recrystallized from benzene and dried under vacuum. PVCL-1 and PVCL-2 were prepared through radical polymerization in benzene (70 °C) using AIBN as initiator. Briefly, recrystallized VCL (0.5 g) was added to a flask filled with argon and anhydrous benzene. After equilibration at 70 °C, AIBN was added drop-wise and the reaction was allowed to proceed for 12 or 24 h and then the product was precipitated in cold hexane. The precipitate was filtered and dried under vacuum overnight. For preparation of PVCL-3, the initiator VA-057 was added to a flask filled with argon and DI water. After equilibrating at 55 °C, a solution of recrystallized VCL in DI water was injected into the flask and allowed to react for a 24 h. The reaction mixture was precipitated in cold ethanol, dialyzed against DI water, and then lyophilized.

2.1.2. ^{1}H NMR

^{1}H NMR spectroscopy was carried out using a Bruker 400 MHz NMR spectrometer. Samples were dissolved in deuterated chloroform ($CDCl_3$) or deuterated water (D_2O) at room temperature.

2.1.3. Thermogravimetric Analysis (TGA)

TGA was performed using a TA Instrument TGA Q50 (New Castle, DE) under nitrogen atmosphere at heating rates of 20 °C · min^{-1}.

2.1.4. Measurements of Phase Transition Temperatures

Photometry measurements were carried out using a SpectraMax Plus 384 plate reader at wavelength 480 nm using a sample concentration of 2.5% (w/v) in Millipore water.

2.1.5. Size Exclusion Chromatography (SEC)

Polymer samples were analyzed using the Malvern Viscotek Triple Detection SEC system. The bulk PVCL was dissolved in *N*-methylpyrrolidone (NMP) at 50 °C for 3–5 h to make a 4 mg · mL^{-1} solution. NMP was used as the mobile phase with a flow rate of 0.5 mL · min^{-1} and a column/detector temperature was set at 60 °C and lithium bromide was used to increase the solubility. All PVCL samples were calibrated against polystyrene standards.

2.1.6. Electrospinning

The electrospinning apparatus consisted of syringe pumps (New Era pump systems Inc., NY), a high voltage supply (Spellman, CZE 1000R, High Voltage Electronics Corporation, NY) and a spinneret to which a single was attached. PVCL fibers were electrospun from ethanol or water solutions, collected on grounded aluminum foil, and dried in vacuum oven. PVCL/CA composite fibers were electrospun from dimethylformamide (DMF) solution and collected on to a pair of parallel aluminum sheets as grounded electrodes. Briefly, PVCL (8%), CA (8%), and poly(ethylene oxide) (2%) were dissolved in DMF and allowed to mix for 15 min at 100 °C. This homogeneous mixture was electrospun into nanofibers and then treated with 0.1 N NaOH solution at 100 °C for 3 h to produce the regenerated PVCL/cellulose bi-component films.

2.1.7. Scanning Electron Microscopy (SEM)

Samples were imaged using a field emission scanning electron microscope (FE-SEM) JSM-6335 (Tachikawa, Tokyo, Japan). All samples were sputter-coated with 10 Å of gold/palladium (Denton Desk II, Moorestown, NJ) prior to imaging. Images were obtained at a working distance of 15 cm using an acceleration voltage of 5–10 kV. The size distribution of PVCL fibers was analyzed by Image J from http://rsbweb.nih.gov/ij/.

2.1.8. Attenuated Total Reflectance Fourier-Transform Infrared Spectroscopy (ATR-FTIR)

ATR-FTIR of the PVCL fiber mats was obtained using a Nicolet Magna-IR 550 Series II spectrometer (Nicolet Instrument Corp., Madison, WI). Each measurement had 256 scans with a resolution of $\pm 4\,cm^{-1}$ using a germanium crystal at an incident angle of 45°. The depth of IR penetration at this incident angle is 0.1–1 μm.[14]

2.1.9. Contact Angle Measurements

Static contact angles were measured by using a contact angle goniometer equipped with light source from Schott-Fostec, LLC (Elmsford, NY), and a high-resolution camera from Mightex system. Contact angles were measured by recording the image of a drop of water onto the fiber mat within <5 s of application of the drop. Measurements were done at both room temperature and elevated temperature (40–100 °C).

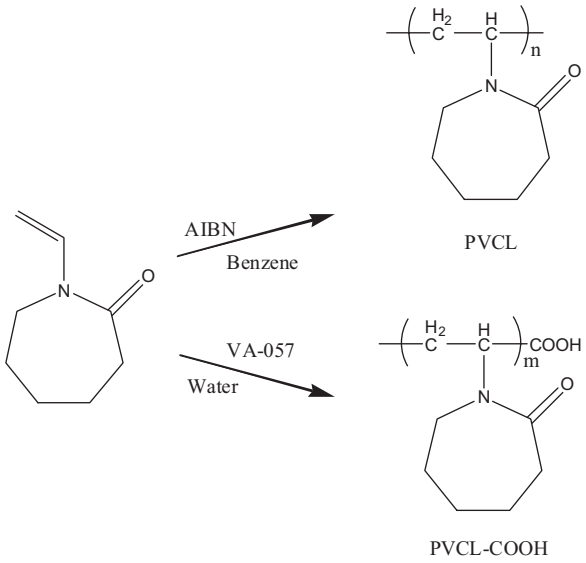

Figure 1. Polymerization of VCL via different methods.

3. Results and Discussion

3.1. PVCL Synthesis and Characterization

PVCL was prepared by free radical polymerization at different monomer feed concentrations, initiators (AIBN and VA-057), and solvents (benzene and water) (Figure 1). A group of PVCL homopolymers with various molecular weights and terminal functional groups were produced. The neutral initiator AIBN was employed in benzene to afford PVCL-1 and PVCL-2, whereas a water-soluble initiator VA-057 was utilized to produce PVCL-3 with COOH at the terminal(s) of polymer chain. A summary of reaction conditions and resultant homopolymers are listed in Table 1 and 2.

PVCL homopolymers were characterized by ^{1}H NMR and FTIR. The assignment of proton peaks (Figure S1 of Supporting Information) for monomer VCL and polymer PVCL-3 is as follows: ^{1}H NMR of VCL in $CDCl_3$: 7.5–7.4 (1H, m, N−C*H* vinyl group), 4.3–4.2 (2H, m, CH_2 vinyl group), 3.3 (2H, t, N−CH_2 caprolactam ring), 2.25 (2H, t, COCH_2 caprolactam ring), 1.4–1.2 (6H, m, CH_2 caprolactam ring). ^{1}H NMR PVCL-3, $CDCl_3$: 4.5–4 (1H, b, N–C*H* backbone), 3.5–3.0 (2H, b, N−CH_2 caprolactam ring), 2.5–2.0 (2H, b, COCH_2 caprolactam ring),

Table 1. Summary of reaction conditions.

Polymer	Solvent	[VCL] [mol L^{-1}]	[Initiator] [mmol L^{-1}]	*T* [°C]	Reaction time [h]
PVCL-1	benzene	0.028	64	70	22
PVCL-2	benzene	0.014	30	70	14
PVCL-3	H_2O	0.014	15.9	55	21

Table 2. Physical parameters of PVCL homopolymers prepared in organic and aqueous solvents.

Polymer	$\overline{M}_n$ [g mol^{-1}]	$\overline{M}_w$ [g mol^{-1}]	PDI	[*n*] [dL g^{-1}]	R_H[a)] [nm]	MHS[b)]
PVCL 1	17 000	38 050	2.24	0.13	4.00	0.77
PVCL 2	21 200	48 550	2.29	0.15	4.70	0.67
PVCL 3	192 500	948 250	4.93	0.79	19.80	0.58

[a)]Hydrodynamic radius; [b)]Mark-Houwink-Sakurada parameter (a relation between intrinsic viscosity and molecular weight).

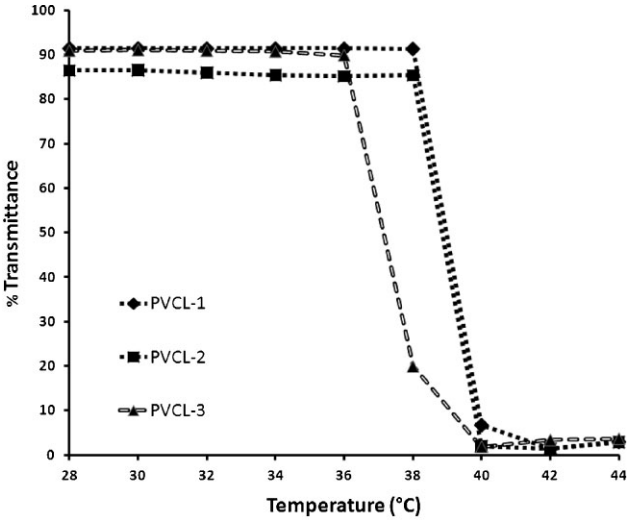

Figure 2. Phase transition temperature measurements of 2.5% (w/v) PVCL in water.

2.0–1.0 (8H, b, CH_2 backbone and caprolactam). The disappearance of the vinyl proton at $\delta = 7.5$ in ^{1}H NMR confirmed no residual monomer in PVCL. In the FTIR, a broad absorption at 3450 cm^{-1} reveals O–H stretching from COOH groups of PVCL-3 (Figure S2c of Supporting Information), and the characteristic absorption peaks at 2924 cm^{-1} (aliphatic C–H stretch), 1631 cm^{-1} (amide I), 1480 cm^{-1} (alpha C–N stretch), and 1350–1500 cm^{-1} (C–H deformation) also confirm the PVCL homopolymers.

The phase transition temperature was determined by recording the percentage of transmittance of 2.5% (w/v) PVCL aqueous solutions over a range of temperatures (Figure 2). The inflection points of PVCL-1 and PVCL-2 (40 °C) were slightly higher than that of PVCL-3 (37–38 °C), which is consistent with the Flory-Huggins relationship as PVCL-3 has a much higher molecular weight compared to the other two polymers.[15,16]

3.2. Electrospinning and Characterization of PVCL Homopolymers

Solvent preference was among the important parameters impacting the preparation of PVCL electrospun fibers. Ethanol and water were good solvents for electrospinning PVCL homopolymers (Table 3). However, due to the differences in R_H and viscosity (Table 2) for each PVCL, ethanol was the most favorable solvent for electrospinning. The less polar ethanol solvent may have diminished the intermolecular hydrophobic interactions between PVCL and solvent allowing less coil-to-globule transitions during the electrospinning process.

The electrospinning parameters are listed in Table 3 for preparation of the PVCL fibers and PVCL/CA composite fibers. As expected, PVCL-1 with lowest molecular weight among three homopolymers had the highest threshold spinnable concentration in ethanol (65%). The resulting electrospun fibers from ethanol had a broad size distribution (Figure 3). No fibers were ever obtained from PVCL-1 water solutions even though many possible concentrations were examined.

PVCL-2 electrospun fibers (Figure 4) were prepared from three concentrations in ethanol 35, 45, and 65% w/v. The uniform fibers with few beads were produced from 35%

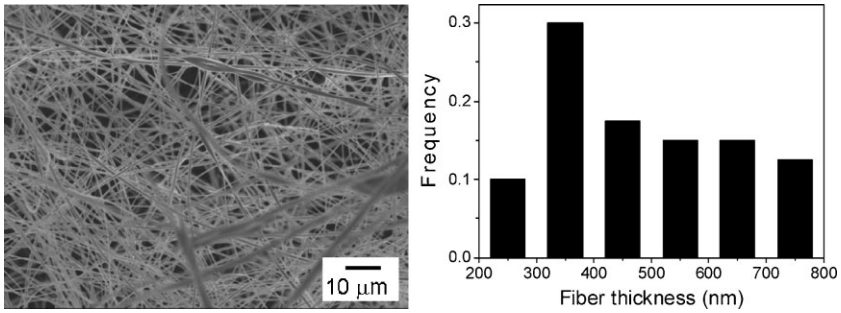

Figure 3. FE-SEM images of: (a) PVCL-1 and (b) size distribution of PVCL-1 nanofibers.

Table 3. Summary of electrospinning conditions.

Sample	Solvent	Concentration [%w/v]	Flow rate [μL min^{-1}]	Voltage [kV]	Height [cm]
PVCL 1	ethanol	65	31	20	12
PVCL 2	ethanol	35	3	17.5	12
PVCL 3	ethanol	35	5	15	12
PVCL 3	water	45	21	20	14
PVCL 1–cellulose acetate-PEO	DMF	8–8–2	25	10	23
PVCL 2–cellulose acetate-PEO	DMF	8–8–2	16	17.5	23
PVCL 3–cellulose acetate-PEO	DMF	8–8–2	16	15.5	23

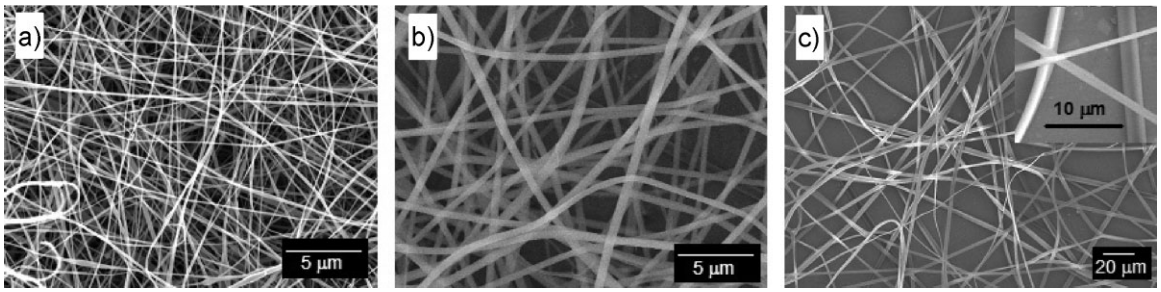

Figure 4. FE-SEM image of PVCL 2 nanofibers: (a) PVCL-2 35% (w/v) in ethanol, (b) PVCL-2 45% (w/v) in ethanol, and (c) PVCL2-65% (w/v) in ethanol.

ethanol with an average fiber diameter of 137 nm. Increasing the concentration to 45% directly correlated to an increase in fiber average diameter (473 nm). At 65%, the resulting PVCL-2 electrospun fibers revealed a flat fiber morphology with an average size of 2245 nm, which was similar to PNIPAM electrospun fibers prepared from 12% acetone solution.[17]

The formation of ribbon like morphology requires a thin solid film or skin on the jet surface and a relatively low viscosity jet core. The skin on the jet surface is formed by rapid evaporation of concentrated polymer solution at the jet surface during electrospinning, and the core solution evaporation is slowed down and concentric shrinkage of jet via polymer solidification can be avoided. With further evaporation of core solution, the fiber collapses under atmospheric force; therefore a flat ribbon like morphology is formed. However, at low concentrations of polymer solution, the jet has a smaller diameter than at high concentrations; the jet core solution can then be evaporated more efficiently before a skin forms on the jet surface. We suggest that this explains cylindrical shape of the fibers.[18,19]

Field-emission scanning electron microscopy (FE-SEM) images of PVCL-3 fibers electrospun from ethanol and water solutions are shown in Figure 5. PVCL-3 (35%) in ethanol produced mostly wide flat fibers (Figure 5A) that exhibited flat dog bone morphology, similar to PNIPAM fibers electrospun from acetone solutions at 12 and 14% and very thin fibers were also found within the web of flat fibers. Such ribbon-like fibers are not found in PVCL-3 fiber mats prepared from 45% aqueous solution (Figure 5B). On decreasing the PVCL3 concentration in ethanol to 25 and 15%, a narrow dog-bone surface morphology was observed (Figure S5 of Supporting Information).

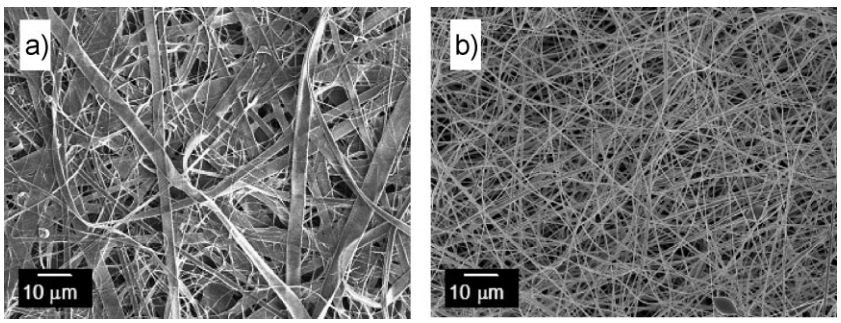

Figure 5. FE-SEM image of PVCL-3 fiber mats: (a) PVCL-3 35% (w/v) in ethanol and (b) PVCL-3 45% in H_2O.

3.3. Electrospinning and Characterization of PVCL/Cellulose Bi-Component Films

Three PVCL-CA composite fibers were electrospun from DMF solution and the spinning conditions were similar to each other (Table 3). PVCL-1-CA non-woven fiber mats showed a whisking orientation with intermittent beads-on-a-string morphology having an average size of 280 nm (Figure 6a and S5a of Supporting Information). PVCL-2–CA fibers mats showed non-woven fiber mats having an average fiber diameter of 326 nm (Figure 6b and S5b of Supporting Information). Straight fibers were found for PVCL-3-CA (Figure 6c) and the average diameter of the composite fiber increased to 573 nm (Figure S5c of Supporting Information). Since concentration of PVCL and CA was kept the same for the three composite fiber mats, the increase of average fiber diameter can be ascribed to the increase of PVCL molecular weight.

The deacetylation of PVCL-CA composite fibers was carried out in 0.1 N NaOH at 100 °C for 3 h. The completion of deacetylation was confirmed by FTIR (Figure 7) as the appearance of the broad peak at ≈3400 cm^{-1} from O–H stretch of cellulose and disappearance of the peak at 1 720 cm^{-1} from C=O stretch of ester group in CA. The presence of PVCL in composite fibers is also confirmed by aliphatic CH and CH_2 absorption around 2900 cm^{-1}. The deacetylation process occurs at 100 °C (well above phase transition temperature of PVCL), however, it was noted that a small fraction of PVCL leached from fiber mats into aqueous solution after ≈1 h deacetylation. The

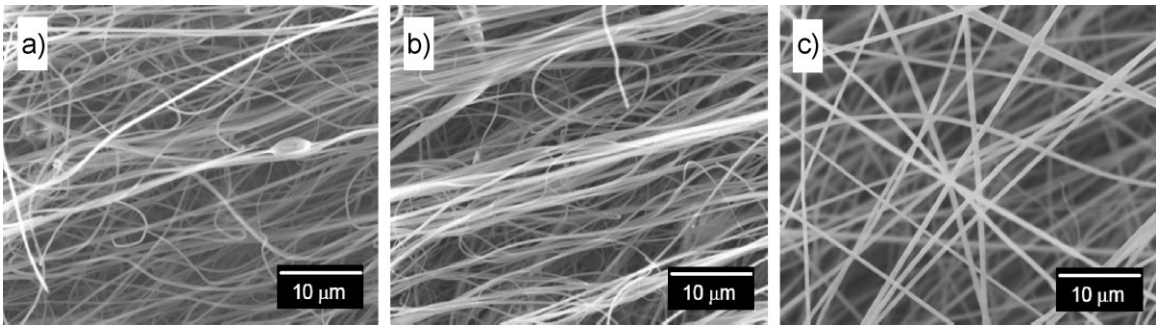

Figure 6. FE-SEM images of PVCL-CA electrospun fiber mats: (a) PVCL-1-CA, (b) PVCL-2-CA, and (c) PVCL-3-CA.

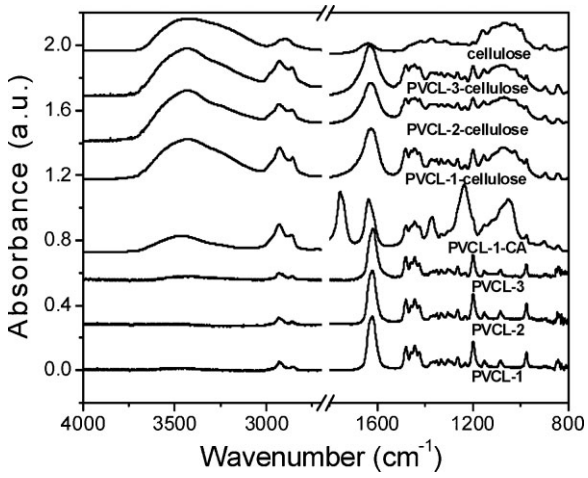

Figure 7. FTIR spectra of (a) cellulose,; (b) PVCL-1-CELL, (c) PVCL-2-CELL, (d) PVCL-3-CELL, (e) PVCL-1, (f) PVCL-2, and (g) PVCL-3.

supernatant was analyzed by FTIR and confirmed to contain PVCL and PEO. Furthermore, FTIR confirmed that PEO was no longer present in PVCL-CELL (cellulose) (Figure 7). Different morphologies were observed for PVCL-CELL and PVCL-CA. SEM images (Figure 8) show that the fibers had dispersed into a continuous film which was caused by partial dissolution of PVCL during hydrolysis, and while fiber drying, the remaining solution on the fiber mat can evaporate and leave a thin film of PVCL on the fiber mat.

The thermo-responsiveness of neat PVCL, CA fiber mats, and composite PVCL-CA fiber mats was measured by contact angle goniometer. It was found that both neat PVCL fiber mats and CA fiber mats (containing 20% PEO) did not show any difference in wettability at temperatures below and above phase transition temperature as water droplet spread instantly on the fiber mats. The PVCL-2-CA fiber mats showed a contact angle of 5° at 20 °C and 133° at temperature ≈40–50 °C (Figure 9a and b). It was also noted that PVCL-1-CA and PVCL-2-CA fiber mats have similar contact angle (data not shown). The chain terminal carboxylic acid group may provide additional hydrophilicity to the PVCL-3-CA fiber mat as for the water droplet applied on PVCL-3-CA fiber had a contact angle lower than that of PVCL-1-CA and PVCL-2-CA. Films of PVCL-2-CA cast from acetone showed lower contact angles at temperatures higher than 40 °C (Figure 9d, contact angle 50°) than PVCL-2-CA fiber mats (Figure 9b, contact angle 133°). In the case of the room temperature measurements, the contact angle on the fiber mat (Figure 9a, contact angle 5°) is much smaller than the contact angle on the film (Figure 9c, contact angle 38°). These observations are due to a lower surface roughness of the PVCL-2-CA films than that present in the PVCL-2-CA fiber mats.

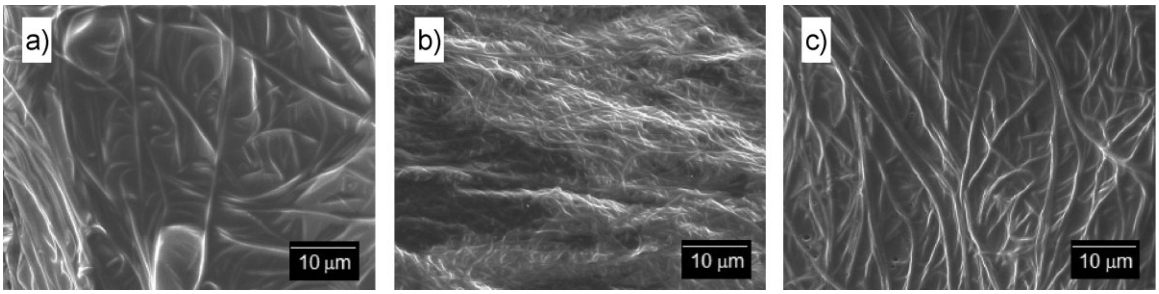

Figure 8. FE-SEM image of PVCL/cellulose bi-component film prepared through alkaline hydrolysis: (a) PVCL-1-CELL, (b) PVCL-2-CELL, and (c) PVCL-3-CELL.

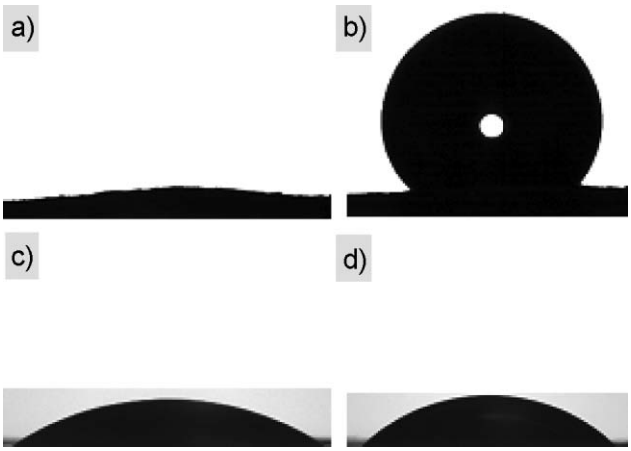

Figure 9. Contact angle measurements: (a) PVCL-2-CA fibers at 20 °C, (b) PVCL-2-CA fibers at 40–50 °C, (c) PVCL-2-CA cast film at 20 °C, and (d) PVCL-2-CA cast film at 40–50 °C.

The thermal behavior of PVCL-CELL bi-component film was characterized by TGA with nitrogen purging (Figure S8 and S9 of Supporting Information). The first step of weight loss from 220 to 365 °C is attributed to cellulose decomposition; the second step of weight loss from 400 to 500 °C corresponds to PVCL degradation.[20] The weight loss occurring at 100–150 °C for PVCL-3 may be due to the evaporation of residual water within the PVCL3 fibers. It was noted that both derivative peaks of cellulose and PVCL-3 in bi-component film are slightly shifted to lower temperatures compared to the neat cellulose and PVCL-3 fibers, which indicates a lower thermal stability in PVCL-3-CA composite fiber (Figure S9 of Supporting Information).

4. Conclusion

Temperature-responsive PVCL was prepared in both organic and aqueous solvents using AIBN and VA-057 as free radical initiators, respectively. The different functionality of each free radical initiators had an effect on the molecular weight of the resultant homopolymers. Fibers were obtained through electrospinning from PVCL homopolymer and PVCL-CA solutions. The morphologies of PVCL homopolymers and PVCL/CA composite fibers were dependent on solution conditions such as solution concentration, viscosity, solvent surface tension, and spinning conditions such as flow rate and applied voltages. The PVCL-1-CA and PVCL-2-CA fiber mats showed higher hydrophobic properties than PVCL-3-CA.

Acknowledgements: The authors thank the financial support from JNC Corporation. Also the authors would like to acknowledge the Rensselaer Polytechnic Institute Nanoscale Science and Engineering Center for Directed Assembly of Nanostructures (NSF Partnerships in Undergraduate Institutions: A12024-01/DMR-0642573) and the Martin Luther King, Jr. Visiting Professorship at Massachusetts Institute of Technology. The authors would also like to thank the Institute of Solider Nanotechnology (ISN) at MIT where research was conducted. Special thanks go to Dr. Jason Suarez at the Malvern Instruments Analysis Laboratory for the analysis of PVCL using Visotek Triple detector system. Additional thanks are given to Professor Chang Ryu of the RPI Chemistry Department for assisting us in making the contact angle measurements.

Received: March 8, 2012; Revised: April 26, 2012; Published online: August 14, 2012; DOI: 10.1002/mame.201200081

Keywords: electrospinning; morphology; nanotechnology; temperature-responsive; thermo-gravimetric analysis

[1] N. Bhardwaj, S. C. Kundu, *Biotechnol. Adv.* **2010**, *28*, 325.
[2] I. Y. Galaev, B. Mattiasson, *Trends Biotechnol.* **1999**, *17*, 335.
[3] I. Galaev, "*Smart Polymers: Applications in Biotechnology and Biomedicine*.", 2nd edition, (Ed: I. Galaev), CRC Press, Boca Raton **2007**.
[4] Y. Maeda, T. Nakamura, I. Ikeda, *Macromolecules* **2002**, *35*, 217.
[5] A. A. Vikhrov, E. A. Markvicheva, T. Y. Mareeva, S. V. Khaidukov, V. A. Nesmeyanov, M. N. Manakov, J. L. Goergen, A. Marc, V. P. Zubov, *Biotechnol. Technol.* **1998**, *12*, 11.
[6] E. A. Markvicheva, V. I. Lozinsky, F. M. Plieva, K. A. Kochetkov, L. D. Rumsh, V. R. Zubov, J. Maity, R. Kumar, V. S. Parmar, Y. N. Belokon, *Pure Appl. Chem.* **2005**, *77*, 227.
[7] J. Ricka, M. Meewes, R. Nyffenegger, T. Binkert, *Phys. Rev. Lett.* **1990**, *65*, 657.
[8] I. Dimitrov, B. Trzebicka, A. H. E. Muller, A. Dworak, C. B. Tsvetanov, *Prog. Polym. Sci.* **2007**, *32*, 1275.
[9] K. Van Durme, H. Rahier, B. Van Mele, *Macromolecules* **2005**, *38*, 10155.
[10] H. Vihola, A. Laukkanen, L. Valtola, H. Tenhu, J. Hirvonen, *Biomaterials* **2005**, *26*, 3055.
[11] A. Laukkanen, L. Valtola, F. M. Winnik, H. Tenhu, *Macromolecules* **2004**, *37*, 2268.
[12] H. Vihola, A. K. Marttila, J. S. Pakkanen, M. Andersson, A. Laukkanen, A. M. Kaukonen, H. Tenhu, J. Hirvonen, *Int. J. Pharm.* **2007**, *343*, 238.
[13] V. Boyko, A. Pich, Y. Lu, S. Richter, K. F. Arndt, H. J. P. Adler, *Polymer* **2003**, *44*, 7821.
[14] B. Kaeselev, J. Pieracci, G. Belfort, *J. Membr. Sci.* **2001**, *194*, 245.
[15] F. Meeussen, E. Nies, H. Berghmans, S. Verbrugghe, E. Goethals, F. Du Prez, *Polymer* **2000**, *41*, 8597.
[16] F. Masoumeh, S. Khoee, M. Zarrabi, *J. Appl. Polym. Sci.* **2008**, *109*, 597.
[17] D. N. Rockwood, D. B. Chase, R. E. Akins, J. F. Rabolt, *Polymer* **2008**, *49*, 4025.
[18] S. Y. Tsou, H. S. Lin, C. Wang, *Polymer* **2011**, *52*, 3127.
[19] S. Koombhongse, W. X. Liu, D. H. Reneker, *J. Polym. Sci., Part B: Polym. Phys.* **2001**, *39*, 2598.
[20] S. Kozanoglu, T. Ozdemir, A. Usanmaz, *J. Macromol. Sci., Part A: Pure Appl. Chem.* **2011**, *48*, 467.